STRUCTURE NOTE

Structure of YciI from *Haemophilus influenzae* (HI0828) Reveals a Ferredoxin-Like α/β-Fold with a Histidine/Aspartate Centered Catalytic Site

Mark A. Willis,[1] **Feng Song,**[2] **Zhihao Zhuang,**[2] **Wojciech Krajewski,**[1] **Vani Rao Chalamasetty,**[3] **Prasad Reddy,**[3] **Andrew Howard,**[4,5] **Debra Dunaway-Mariano,**[2] **and Osnat Herzberg**[1]*

[1]*Center for Advanced Research in Biotechnology, University of Maryland Biotechnology Institute, Rockville, Maryland*
[2]*Department of Chemistry, University of New Mexico, Albuquerque, New Mexico*
[3]*The National Institute of Standards and Technology, Gaithersburg, Maryland*
[4]*Advanced Photon Source, Argonne National Laboratory, Argonne, Illinois*
[5]*Biological, Chemical, and Physical Sciences, Illinois Institute of Technology, Chicago, Illinois*

Introduction. The 11-kDa protein is encoded by the HI0828 gene of *Haemophilus influenzae* (YciI) targeted by the Structure to Function Structural Genomics Project (http://s2f.carb.nist.gov) as a prototype of a novel sequence family of unknown fold and biochemical function. Here we report the 0.99 Å crystal structure of the HI0828 dimer, which defines an α/β ferredoxin-like fold. A probable active site is identified, in which an invariant histidine residue is observed complexed to $ZnCl_3$. Biochemical function was tested using a focused substrate activity screen that was designed using the active-site structure and assuming the participation of an invariant histidine–aspartate pair in catalysis.

Methods. *Protein production.* The gene encoding HI0828 was amplified from *H. influenzae* KW20 genomic DNA and cloned into pET15b (Novagen), which contains a thrombin-cleavable N-terminal His_6-tag. Selenomethionine-substituted protein expression was induced in *Eshcerihcia coli* B834 (DE3) cells cultured at 37°C with IPTG (0.4 mM final concentration) when the cell density in LB growth media (with 100 μg/mL ampicillin) reached $A_{600} = 0.6$. The protein was purified using a Ni-NTA column (Qiagen). The N-terminal His_6-tag was cleaved with thrombin, and the cleaved protein was separated from uncleaved protein on a second Ni-NTA column as described for the protein HI0442.[1] Finally, the buffer was exchanged for 20 mM Na^+ HEPES and 2 mM imidazole (pH 7.0), 5 mM NaCl, 0.1 mM EDTA, and 0.1 mM DTT. The molecular weight of the protein and the extent of selenomethionine incorporation were determined by MALDI-TOF mass spectroscopy.

Structure determination. Crystals of HI0828 belonging to space group $P2_12_12_1$ (with cell dimensions of $a = 42.5$ Å, $b = 63.3$ Å, $c = 75.5$ Å, and a single dimer in the asymmetric unit) appeared in a few days at room temperature in hanging-drop vapor diffusion experiments using equal volumes of protein (11 mg/mL), and well solution (16% PEG 4000, 0.1 M Na^+ cacodylate, pH 5.5, 20 mM Zn^{+2} acetate, 2% dioxane). Diffraction data were collected around the selenium absorption edge at 100 K on cryoprotected crystals (using a coating of perfluoropolyether oil, MW = 2800, in combination with crystallizing solution adjusted to 19% PEG 4000, and 15% PEG 400) on the IMCA-CAT beamline 17-ID at the Advanced Photon Source, Argonne National Laboratory, Argonne, IL (Table I).

Diffraction data were processed with the HKL Suite[2] and scaled using XPREP.[3] Heavy atom sites were found by the program SOLVE[4] using data to 1.5 Å. The SOLVE phases were modified by RESOLVE[5] and used to produce a high-quality electron density map into which the model was automatically built by ARP/wARP.[6] Only eight of the dimer's 200 residues required manual building using the program O.[7] Of the three remaining residues after His-tag cleavage (Gly-Ser-His), two were visible in the electron density map (Ser-His). Refinement of the model using $λ_1$ (maximum f′) data was carried out initially using CNS[8] and finally with SHELX-97.[9] Ordered water molecules were included in the model along with zinc and chloride ions, a cacodylate molecule, and two polyethylene glycol molecules. The assignment of zinc ions is consistent with the requirement for this metal in the crystallization solution and with the anomalous difference maps calculated with data collected at the Se and Hg edge energies. The identities of the chloride ions were confirmed by anomalous and dispersive difference maps calculated using selenomethionine/Hg combined MAD, bromide MAD (in which bromide substitutes for chloride), and iodide SAD (in

TABLE I. Crystallographic Data and Refinement Statistics

Space group	$P2_12_12_1$			
Cell dimensions (Å)	$a = 42.5$, $b = 63.3$, $c = 75.5$			
No. of dimers/asymmetric unit	1			
Data sets	λ_1	λ_2	λ_3	λ_4
	Se peak	Se edge	Se high energy	Se low energy
Wavelength (Å)	0.9793	0.9795	0.9664	0.9832
Resolution (Å)	20–0.99	20–1.15	20–1.3	20–1.3
No. of Observations	1,042,859	748,894	341,043	330,135
Unique Reflections[a,b]	206,417	137,392	88,424	86,574
Completeness (%)[b]	94.2 (83.4)	97.3 (96.7)	91.5 (78.4)	89.6 (69.6)
R_{sym} (I)[b,c]	0.063 (0.216)	0.066 (0.376)	0.048 (0.228)	0.048 (0.223)
I/σ[b]	16.7 (6.0)	14.8 (5.1)	16.1 (4.5)	16.5 (4.3)
Model and refinement statistics				
Resolution (Å)	15–0.99			
Wavelength (Å)	0.9793			
Unique reflections ($F > 0$)	107,935			
Completeness (%)	95.0			
R_{cryst}[d]	0.109			
R_{free}[d]	0.132			
No. of protein atoms	1705			
No. of water molecules	329			
No. of other atoms	38			
RMSD from ideal geometry				
Bond Lengths (Å)	0.014			
Bond Angle Distances (Å)	0.032			
Ramachandran Plot (%)[e]			Average B-factor (Å^2)	
Most favored	90.9		Molecule A	11
Allowed	8.0		Molecule B	14
Generously allowed	1.1		Water	29
Disallowed	0.0		Other atoms	22

[a]Friedel pairs are treated as independent reflections.
[b]For reflections with I > 0. Values in parentheses are for the highest resolution bins (1.10–0.99 Å for λ_1 data, 1.25–1.15 Å for λ_2 data, and 1.4–1.3 Å for the λ_3 and λ_4 data).
[c]$R_{sym} = \Sigma_{hkl}[(\Sigma_i |I_i - \langle I \rangle|)/\Sigma_i |I_i|]$.
[d]$R_{cryst} = (\Sigma_{hkl}||F_{obs}| - k|F_{calc}||/\Sigma_{hkl}|F_{obs}|)$ calculated for all reflections used in the final refinement step. R_{free} is calculated for a randomly selected 5% set of reflections not included in the refinement.
[e]Analyzed using ProCheck[30].

which two iodides substitute for three chlorides). Near completion of the refinement, anisotropic displacement parameters were refined, after which hydrogen atoms were added. In a final step, the previously omitted test set reflections were included to calculate a final *R*-factor (for validation, the same 5% random test set of data was omitted from refinement in CNS and SHELX-97). Model refinement statistics are shown in Table I. The figures were prepared with PyMOL (DeLano Scientific).

Substrate activity assays. Activity assays were carried out with native HI0828 prepared by expression of HI0828/pET-23b in *E. coli* BL21 (DE3) followed by purification on DEAE-Sepharose and Sephacryl-S-200 columns at 4°C. All substrates were obtained from commercial sources, with the exception of potassium oxirane carboxylate, which was a gift from Dr. Chris Whitmann. Assay solutions were buffered at 25°C with 50 mM K$^+$ HEPES (pH 7.5) in the presence and absence of 0.2 mM ZnCl$_2$ and 1 mM MgCl$_2$. HI0828 (25–150 μM) and substrate (0.05–50 mM) were reacted for up to 2 h. Phosphate ester hydrolysis was monitored spectrophotometrically at 360 nm ($\Sigma\varepsilon = 9.0$ mM^{-1}cm^{-1}) using the EnzChek phosphate assay kit (Molecular Probes) or, in the case of the *p*-nitrophenylphosphate substrate, directly at 405 nm ($\Delta\varepsilon = 16.7$ mM^{-1}cm^{-1})[10]. Acyl-CoA thioesterase activity was monitored using the 5,5′-dithio-bis(2-nitrobenzoic acid)-based spectrophometric assay described previously, or in the

case of 4-hydroxybenzoyl-CoA, determined directly by the absorbance change at 300 nm ($\Delta\varepsilon = 11.8$ mM^{-1}cm^{-1}).[11] Hydrolyses of 4-nitrophenylesters and glycosides were monitored by absorbance change at 405 nm ($\Delta\varepsilon = 16.7$ mM^{-1}cm^{-1}). Other reactions were monitored by HPLC or ^{1}H NMR.

Site-directed mutants. Mutagenesis was carried out using a PCR-based strategy with HI0828/pET-23b serving as a template, synthetic primers from Invitrogen, the PCR kit from Stratagene, and the thermocycler from TECHNE. Mutant proteins were purified using the same procedure used with the recombinant wild-type HI0828.

Results and Discussion. *Structure.* The 98-amino acid HI0828 monomer has an α/β ferredoxin-like fold with a four-stranded antiparallel β-sheet packed against two kinked α-helices [Fig. 1(A)]. A DALI[12] search identified muconolactone isomerase (MLI)[13] as the closest match (with *Z*-score of 7.7 and an RMSD of 2.8 Å for 82 aligned α-carbon atoms), although the two proteins do not exhibit significant sequence homology (12% over the structurally aligned residues).

HI0828 molecules associate into dimers consistent with dynamic light scattering results (data not shown), and define a subunit interface similar to that of the dimer interface of two MLI protomers (unlike HI0828, the MLI dimers assemble in a pentameric ring, forming a
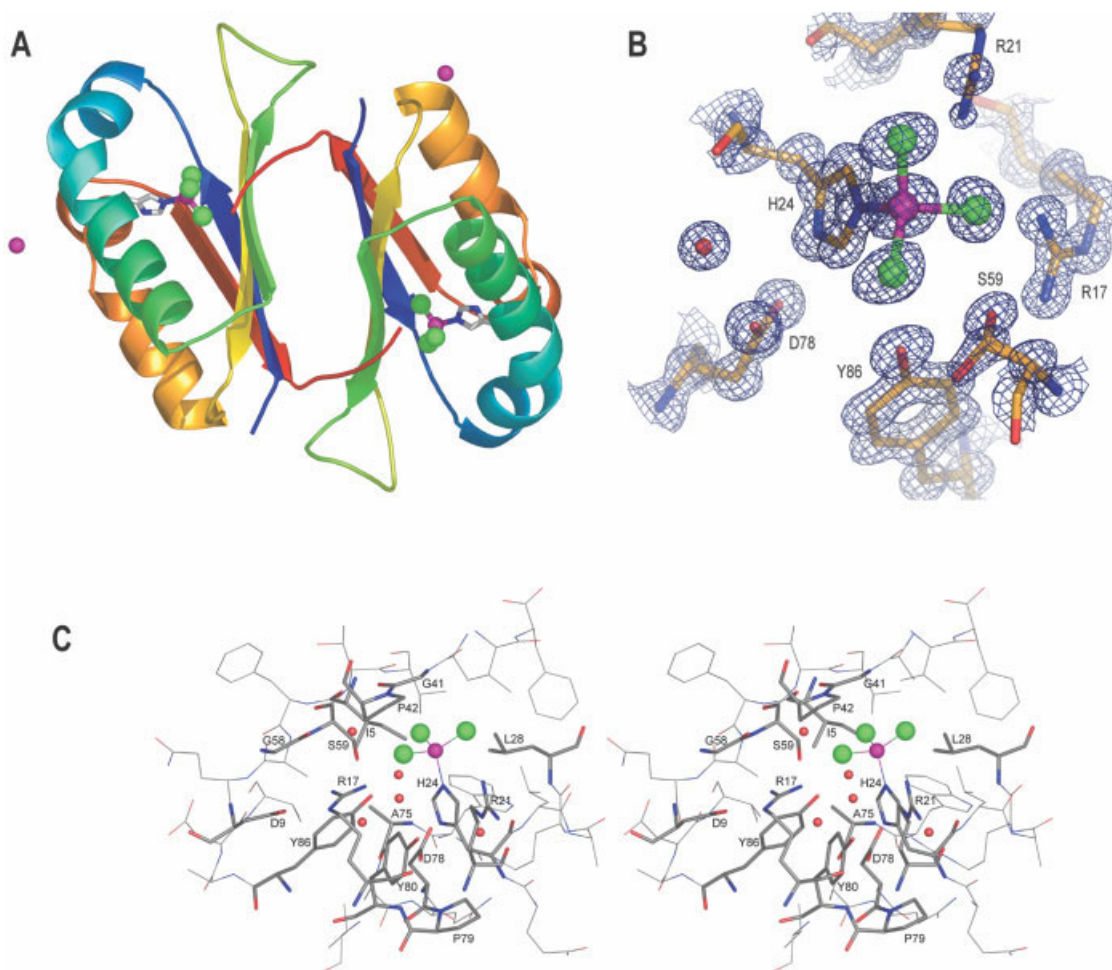
Fig. 1. Structure of HI0828. (**A**) Ribbon diagram of the dimeric protein. The coloring shows the progression of the polypeptide chain from the N-terminus (blue) to the C-terminus (red). The invariant His24 and the coordinated $ZnCl_3$ are shown as sticks and spheres. Two additional zinc ions that mediate dimer–dimer packing are shown as spheres. (**B**) $2F_o–F_c$ electron density (contoured at 1.5 σ) associated with His24, the $ZnCl_3$ adduct (zinc in magenta, chloride in green), and some of the surrounding conserved residues. Ser59 adopts two alternate conformations; Arg21 is shown in one of three alternate conformations. For clarity, some water molecules are not displayed. (**C**) Stereoscopic view of the postulated active site pocket containing the His24–$ZnCl_3$ complex and five water molecules. The conserved residues are labeled and shown with thick bonds. Atoms are indicated by color as follows: carbon (gray), nitrogen (blue), oxygen (red), zinc (magenta), and chloride (green). The water molecules are shown as small red spheres.

decamer),[13] and to that of ActVA-Orf6 monooxygenase (superposition with DALI yields a Z-score of 4.4, an RMSD value of 3.5 Å, and a 9% sequence identity for 77 aligned α-carbon atoms).[14] Recently, a structure of a protein of unknown function from *Thermus thermophilus* Hb8 with a MLI-like fold was submitted to the PDB (Ebihara et al., entry code 1VDI). As with MLI, it exhibits a pentameric ring, and two domains, formed by a single polypeptide chain, replace the homodimer assembly of MLI. Superposition of the N-terminal domain and HI0828 yields Z-score of 4.4, an RMSD value of 2.9 Å, and a 4% sequence identity over 75 aligned residues, and the superposition of the C-terminal domain yields a Z-score of 3.6, an RMSD of 3.1 Å, and a 7% sequence identity over 72 aligned residues.

The two HI0828 molecules in the asymmetric unit are very similar, with a main-chain atom RMSD of 0.32 Å. The largest deviations occur in the first two turns of helix 1 [sky blue helix in Fig. 1(A)] and in the loop connecting β-strands 2 and 3 [yellow loop in Fig. 1(A)].

A surface depression extending into a largely sequestered, solvent-filled, pocket is formed at the edge of the α- and β-layers. This crevice is lined with residues conserved in all HI0828 family members identified by Psi-BLAST analysis[15] (Arg17, Arg21, His24, Gly41, Pro42, Ser59, Asp78, Pro79, Tyr80, and Tyr86), indicating that the pocket and associated residues are the functional center of the molecule [Fig. 1(C)]. Among these residues is the invariant His24, which is seen in the structure coordinated to a tetrahedral $ZnCl_3$ via the N^ε atom (2.0 Å). This arrangement is stabilized through interactions of the guanidinium groups of Arg17 and Arg21 with the chloride ligands [Fig. 1(B)]. The His24 N^δ atom interacts with Asp78, located behind His24 in the pocket [Fig 1(C)]. The His24–Asp78 might function as a catalytic diad, in which the basicity and nucleophilicity of the histidine's imidazole is enhanced by the aspartic acid's carboxylate group.

We have analyzed the structural relationship between HI0828 and MLI further to obtain clues about function.

Although the MLI structure is incomplete (3.3-Å resolution with only the α-carbon atom coordinates available in the PDB),[13] there are interesting similarities between the two proteins beyond the dimeric association. First, as in HI0828, the postulated active site is located along the edge of the α/β sandwich on the side of Helix 1. Second, the C-terminus of the adjacent dimer molecule forms part of the active site in both structures. However, the identities of the active site residues are different. The position occupied by His24 in HI0828 is occupied by a glutamic acid (Glu27) in MLI, a residue that has been proposed to play a role in MLI catalysis.[13] There is no MLI equivalent to the HI0828 Asp78. Instead, two residues located on the C-terminus of the neighboring molecule were proposed to be involved in MLI catalysis, His87 and Ser89. The equivalent C-terminus in HI0828 contributes hydrophobic residues not likely to play a catalytic role. Therefore, MLI and HI0828 represent yet another example of a structure superfamily sharing the same scaffold and active-site location but evolving to perform different catalytic reactions. It is interesting to note that, in addition to the isomerase activity, MLI enzymes exhibit muconolactone dechlorination activity,[16,17] and one family member is a dechlorinase with no isomerase activity.[18] The structural relationship of HI0828 and MLI is reminiscent of another enzyme superfamily that shares the same fold and catalyzes several reactions including isomerization, elimination, and dechlorination. The superfamily members γ-hexachlorocyclohexane dehydrochlorinase (LinA) and scytalone dehydratase, both utilize a His–Asp for proton abstraction, and 3-oxo-Δ^5-steroid isomerase utilizes a Tyr-Asp pair for isomerization.[19]

Function. Because of its limited size, the HI0828 active site may bind only a single reactant, unless one of the reactants is a water molecule. The His24–ZnCl$_3$ coordination observed in the HI0828 structure is reminiscent of the His–AlF$_3$ coordination observed in the crystal structure of nucleoside diphosphate kinase, an enzyme that catalyzes phosphoryl transfer that proceeds via a phosphohistidine intermediate.[20] We tested His24 phosphorylation by reaction with excess phosphoroamidate[21] at pH 8.3 and 37°C for 3 h. Whereas, the thrombin-cleaved His-tagged protein that contains an N-terminal histidine residue (replacing Met1) was phosphorylated at His to form a stable adduct (^{31}P NMR resonances at −4.42 ppm), the native enzyme, which contained only the His24 was not. This result casts doubt on the role of His24 as a mediator of phosphoryl transfer between a donor–acceptor pair but does not rule out His24 function in phosphate ester hydrolysis. Phosphatase activity was probed by testing catalyzed hydrolysis of *p*-nitrophenylphosphate, a slow substrate for many phosphatases, as well as a variety of natural phosphate esters and anhydrides (*p*-nitrophenylphosphate di(amino-2-ethyl-1,3-propanediol, α- and β-D-glucose 1-phosphate, D-glucose 6-phosphate, α-D-glucose 1,6-diphosphate, D-fructose 1,6-diphosphate, D-mannose 6-phosphate, α-D-mannose 1-phosphate, 6-phosphogluconate, DL-α-glycerophosphate, PEP, phosphoserine, phosphothreonine, ADP, and ATP). No activity was observed, and

therefore other hydrolase activities were tested. HI0828 did not catalyze the hydrolysis of acyl or aryl-coenzyme A thioesters, nor did it catalyze the hydrolysis of *p*-nitrophenylglycosides [4-hydroxybenzoyl-CoA, acetyl-CoA, *n*-butyryl-CoA, *n*-hexanoyl-CoA, *n*-octanoyl-CoA, *n*-decanoyl-CoA, methylmalonyl-CoA, glutaryl-CoA, crotonyl-CoA, 3-hydroxy-3-methylglutaryl-CoA, isobutyryl-CoA, β-hydroxybutyryl-CoA, arachidoyl-CoA, stearoly-CoA; *p*-nitrophenyl (β-D-glucopyranoside, β-D-lactopyranoside, α-D-galactopyranoside, β-D-fucopyranoside, α-L-fucopyranoside, and β-L-fucopyranoside)]. No esterase activity was observed towards acetoxyacetate, 3-acetoxypropionate, and 2-(methacryloyloxy)-ethyl phosphate). A low level of hydrolase activity ($\sim 1 \times 10^{-4}$ s^{-1}) was observed with the *p*-nitrophenyl esters of acetate, propionate, butyrate, valerate, and guanidinobenzoate; however, the HI0828 active site mutants H24A and S59A retained 30 and 100% activity, respectively, thus ruling out catalysis by the HI0828 postulated active site. Last, we tested epoxide hydrolysis using oxirane carboxylate (CH$_2$(O)CHCOO—) as substrate but observed no reaction, and we tested hydrolytic dehalogenation in 2-chlorobutyric acid, 2-bromobutyric acid, and 3-bromopropionic acid, but observed no activity.

The uniqueness of the arrangement of active-site residues was demonstrated by carrying out a searches of the PDB using SPASM[22] and PINTS[23] for proteins with a similar catalytic site structure. Various combinations of His24 with Ser59, Asp78, Tyr86, Arg21, Tyr80, Gly41, and Pro42 were examined (the last two residues because they pack against the top of the ZnCl$_3$ cluster). In short, no revealing matches were made with enzymes in which the residue cluster occurs within the catalytic site.

Finally, we turned to examination of sequence homologs and gene context for clues of function. A Psi-BLAST search[15] revealed more than 200 sequences (mostly bacterial and a few fungal), 65 of which are contained in the nonredundant environmental samples database (env_nr). The HI0828 sequence family is listed under Pfam[24] as PF03795 and under INTERPRO[25] as IPR005545, with the common family name given as YCII after the *E. coli* homolog YciI. Only one family member has a characterized activity, and that is the dechlorinase encoded by the *tft*G gene (SwissProt accession # Q45075) of the operon responsible for 2,4,5-trichlorophenoxyacetic acid degradation to maleylacetate[26] in *Burkholderia cepacia*. The dechlorinase, which catalyzes the elimination of HCl in 5-chlorohydroxyquinol to form 2-hydroxy-1,4-benzoquinone, shares 30% sequence identity with HI0828 and conserves the active site His24 and Asp78 diad, which might function in proton abstraction. Is HI0828 a dehalogenase? Its gene context and those of its closest sequence homologs (YciI) would suggest that it is not. The genes encoding HI0825, HI0826, HI0827, HI0828, and HI0829 are separated by only a few nucleotides (gaps of 5, −1, 15, and 16 nucleotides, respectively), and therefore, these proteins are likely to be cotranscribed. HI0825 encodes a membrane protein of unknown function that was assigned a COG2244, "a

general function prediction only" COG said to be involved in the export of O-antigen and teichoic acid.[27] HI0826 is a member of the intracellular septation protein A family (IspZ), and HI0827 (YciA) is a hotdog fold acyl-CoA thioesterase (Willis et al., PDB entry code 1yli). Following HI0828, HI0829 is a putative lytic murein transglycosylase. Hence, the gene context of this cluster indicates relationship to cell structure. In some other bacteria, the HI0828 homolog gene occurs with the septation protein gene and the thioesterase gene or the BolA gene. BolA, a transcription regulator, is believed to be involved in switching the cell between elongation and septation during cell division,[28] and to regulate the transcription of the cell wall enzymes PBP5 and PBP6.[29] In *Coxiella burnetii*, the BolA domain is fused to the C-terminus of the YciI domain (SwissProt accession # Q83D37). We speculate that HI0828 is an enzyme that catalyzes a reaction in which proton abstraction precedes elimination or isomerization, and that this reaction is one step in a larger biochemical process affecting cell morphology.

REFERENCES

1. Lim K, Tempczyk A, Parsons JF, Bonander N, Toedt J, Kelman Z, Howard A, Eisenstein E, Herzberg O. Crystal structure of YbaB from *Haemophilus influenzae* (HI0442), a protein of unknown function coexpressed with the recombinational DNA repair protein RecR. Proteins 2003;50:375–379.
2. Otwinowski Z, Minor W. Processing of X-ray diffraction data collected in oscillation mode. Methods Enzymol 1997;276:307–326.
3. Sheldrick GM. XPREP Programm zur Datenanalyse: Universität Göttingen; 1997.
4. Terwilliger TC, Berendzen J. Automated MAD and MIR structure solution. Acta Crystallogr D Biol Crystallogr 1999;55(Pt 4):849–861.
5. Terwilliger TC. Maximum-likelihood density modification. Acta Crystallogr D Biol Crystallogr 2000;56(Pt 8):965–972.
6. Perrakis A, Morris R, Lamzin VS. Automated protein model building combined with iterative structure refinement. Nat Struct Biol 1999;6:458–463.
7. Jones TA, Zou JY, Cowan SW, Kjeldgaard M. Improved methods for binding protein models in electron density maps and the location of errors in these models. Acta Crystallogr A 1991;47(Pt 2):110–119.
8. Brunger AT, Adams PD, Clore GM, DeLano WL, Gros P, Grosse-Kunstleve RW, Jiang JS, Kuszewski J, Nilges M, Pannu NS, Read RJ, Rice LM, Simonson T, Warren GL. Crystallography & NMR system: A new software suite for macromolecular structure determination. Acta Crystallogr D Biol Crystallogr 1998;54:905–921.
9. Sheldrick GM, Schneider TR. SHELXL: high resolution refinement. Methods Enzymol 1997;277:319–343.
10. Webb MR. A continuous spectrophotometric assay for inorganic phosphate and for measuring phosphate release kinetics in biological systems. Proc Natl Acad Sci USA 1992;89:4884–4887.
11. Zhuang Z, Gartemann KH, Eichenlaub R, Dunaway-Mariano D. Characterization of the 4-hydroxybenzoyl-coenzyme A thioesterase from *Arthrobacter* sp. strain SU. Appl Environ Microbiol 2003;69:2707–2711.
12. Holm L, Sander C. Protein structure comparison by alignment of distance matrices. J Mol Biol 1993;233:123–138.
13. Katti SK, Katz BA, Wyckoff HW. Crystal structure of muconolactone isomerase at 3.3 A resolution. J Mol Biol 1989;205:557–571.
14. Sciara G, Kendrew SG, Miele AE, Marsh NG, Federici L, Malatesta F, Schimperna G, Savino C, Vallone B. The structure of ActVA-Orf6, a novel type of monooxygenase involved in actinorhodin biosynthesis. EMBO J 2003;22:205–215.
15. Altschul SF, Madden TL, Schaffer AA, Zhang J, Zhang Z, Miller W, Lipman DJ. Gapped BLAST and PSI-BLAST: a new generation of protein database search programs. Nucleic Acids Res 1997;25:3389–3402.
16. Prucha M, Peterseim A, Timmis KN, Pieper DH. Muconolactone isomerase of the 3-oxoadipate pathway catalyzes dechlorination of 5-chloro-substituted muconolactones. Eur J Biochem 1996;237:350–356.
17. Prucha M, Wray V, Pieper DH. Metabolism of 5-chlorosubstituted muconolactones. Eur J Biochem 1996;237:357–366.
18. Moiseeva OV, Solyanikova IP, Kaschabek SR, Groning J, Thiel M, Golovleva LA, Schlomann M. A new modified ortho cleavage pathway of 3-chlorocatechol degradation by *Rhodococcus opacus* 1CP: genetic and biochemical evidence. J Bacteriol 2002;184:5282–5292.
19. Nagata Y, Mori K, Takagi M, Murzin AG, Damborsky J. Identification of protein fold and catalytic residues of gamma-hexachlorocyclohexane dehydrochlorinase LinA. Proteins 2001;45:471–477.
20. Xu YW, Morera S, Janin J, Cherfils J. AlF3 mimics the transition state of protein phosphorylation in the crystal structure of nucleoside diphosphate kinase and MgADP. Proc Natl Acad Sci USA 1997;94:3579–3583.
21. Chambers RW, Khorana HG. Nucleoside polyphosphates. VII.1 The use of phosphoramidic acids in the synthesis of nucleoside-5′ pyrophosphates. J Am Chem Soc 1958;80:3749–3752.
22. Kleywegt GJ. Recognition of spatial motifs in protein structures. J Mol Biol 1999;285:1887–1897.
23. Stark A, Sunyaev S, Russell RB. A model for statistical significance of local similarities in structure. J Mol Biol 2003;326:1307–1316.
24. Bateman A, Birney E, Cerruti L, Durbin R, Etwiller L, Eddy SR, Griffiths-Jones S, Howe KL, Marshall M, Sonnhammer EL. The Pfam protein families database. Nucleic Acids Res 2002;30:276–280.
25. Mulder NJ, Apweiler R, Attwood TK, Bairoch A, Barrell D, Bateman A, Binns D, Biswas M, Bradley P, Bork P, Bucher P, Copley RR, Courcelle E, Das U, Durbin R, Falquet L, Fleischmann W, Griffiths-Jones S, Haft D, Harte N, Hulo N, Kahn D, Kanapin A, Krestyaninova M, Lopez R, Letunic I, Lonsdale D, Silventoinen V, Orchard SE, Pagni M, Peyruc D, Ponting CP, Selengut JD, Servant F, Sigrist CJ, Vaughan R, Zdobnov EM. The InterPro Database, 2003 brings increased coverage and new features. Nucleic Acids Res 2003;31:315–318.
26. Zaborina O, Daubaras DL, Zago A, Xun L, Saido K, Klem T, Nikolic D, Chakrabarty AM. Novel pathway for conversion of chlorohydroxyquinol to maleylacetate in *Burkholderia cepacia* AC1100. J Bacteriol 1998;180:4667–4675.
27. Tatusov RL, Fedorova ND, Jackson JD, Jacobs AR, Kiryutin B, Koonin EV, Krylov DM, Mazumder R, Mekhedov SL, Nikolskaya AN, Rao BS, Smirnov S, Sverdlov AV, Vasudevan S, Wolf YI, Yin JJ, Natale DA. The COG database: an updated version includes eukaryotes. BMC Bioinformatics 2003;4:41.
28. Aldea M, Hernandez-Chico C, de la Campa AG, Kushner SR, Vicente M. Identification, cloning, and expression of bolA, an ftsZ-dependent morphogene of *Escherichia coli*. J Bacteriol 1988;170:5169–5176.
29. Santos JM, Lobo M, Matos AP, De Pedro MA, Arraiano CM. The gene bolA regulates dacA (PBP5), dacC (PBP6) and ampC (AmpC), promoting normal morphology in *Escherichia coli*. Mol Microbiol 2002;45:1729–1740.
30. Laskowski RA, Macarthur MW, Moss DS, Thornton JM. PROCHECK—a program to check the stereochemical quality of protein structures. J Appl Crystallogr 1993;26:283–291.